Biochemical Pharmacology 244 (2026) 117615

Contents lists available at ScienceDirect

Biochemical Pharmacology

journal homepage: www.elsevier.com/locate/biochempharm

# NLRP3 inhibition protects human coronary endothelial cells from oxidative and lipotoxic stress

Astrid Parenti [a,b,*], Costanza Titi [a], Arianna Brovero [c], Federica Blua [d], Francesca Boccato [d], Angela Silvano [a], Francesco Fedele [b,e], Anna Vittoria Mattioli [b,f], Massimo Bertinaria [d], Pasquale Pagliaro [b,c,1], Claudia Penna [b,c,1]

[a] Department of Health Sciences, University of Florence, Italy
[b] National Institute for Cardiovascular Research (INRC), Bologna, Italy
[c] Department of Clinical and Biological Sciences, University of Turin, Italy
[d] Department of Drug Science and Technology, University of Turin, Italy
[e] Department of Clinical, Internal, Anesthesiology and Cardiovascular Sciences, Sapienza University of Rome, Viale del Policlinico, 155, 00161 Rome, Italy
[f] Department of Quality of Life Sciences, University of Bologna-Alma Mater Studiorum, 40126 Bologna, Italy

ARTICLE INFO

*Keywords:*
NLRP3
Endothelial dysfunction
Angiogenesis
Lipotoxicity
Oxidative stress
Caspase-1
IL1β

ABSTRACT

An increased production of reactive oxygen species and elevated levels of free fatty acids are linked to inflammation and vascular endothelial dysfunction. Here, we investigated the effects of two pharmacological inhibitors of the NLRP3 inflammasome, INF150 and INF195, on Human Coronary Artery Endothelial Cells (HCAECs) exposed to hydrogen peroxide ($H_2O_2$) and palmitic acid (PA), to mimic the oxidative and lipotoxic stress underlying endothelial dysfunction.

HCAECs were pre-treated for 15 min with either INF150 or INF195, followed by exposure to increasing concentrations of $H_2O_2$ or PA staring from doses that induce endothelial dysfunction without causing cell death. Cell viability was assessed by MTT assay, while *in vitro* angiogenesis was evaluated through pseudo-capillary formation. NLRP3, caspase-1, and IL-1β levels were quantified by ELISA and pyroptosis by LDH release and gasdermin D cleavage. Additionally, we evaluated the protective effects of the two inhibitors in HCAECs primed with TNF-α and subsequently challenged with PA.

Both inhibitors preserved cell viability under oxidative stress conditions, with INF195 showing greater efficacy. Notably, only INF195 significantly protected HCAECs from both PA and TNF-α + PA-induced injury. Exposure to PA, with or without TNF-α, markedly increased caspase-1 expression and pyroptosis which were rescued by INF195. Furthermore, $H_2O_2$ and PA significantly impaired *in vitro* pseudocapillary formation by HCAECs and HUVECs, considered the gold standard for in vitro angiogenesis assays, an effect counteracted by INF195.

These findings suggest that, under oxidative and lipotoxic stress, NLRP3 inflammasome inhibition −particularly *via* INF195 − supports the maintenance of vascular endothelial homeostasis by preserving cell viability and angiogenic function.

*Abbreviations:* CVD, cardiovascular disease; DAMPs, damage-associated molecular patterns; ECs, endothelial cells; ED, Endothelial dysfunction; FBS, foetal bovine serum; FFAs, free fatty acids; GSDMD, gasdermin D; $H_2O_2$, hydrogen peroxide; HCAECs, Human Coronary Artery Endothelial Cells; HUVECs, human umbilical vein endothelial cells, IL-1β, Interleukin-1 beta; LDH, Lactate dehydrogenase; NADPH, nicotinamide adenine dinucleotide phosphate; NLRP3, NOD-like receptor pyrin domain-containing 3; PA, palmitic acid; PAMPs, pathogen-associated molecular patterns; PRRs, Pattern recognition receptors; ROS, reactive oxygen species; TNF-α, Tumor necrosis factor alpha.

* Corresponding author at: Department of Health Sciences, Clinical Pharmacology and Oncology Section, V. le G. Pieraccini, 6, 50139 Florence Italy.
*E-mail address:* astrid.parenti@unifi.it (A. Parenti).

[1] Equal contribution

https://doi.org/10.1016/j.bcp.2025.117615
Received 4 August 2025; Received in revised form 28 November 2025; Accepted 5 December 2025
Available online 6 December 2025
0006-2952/© 2025 The Authors. Published by Elsevier Inc. This is an open access article under the CC BY license (http://creativecommons.org/licenses/by/4.0/).

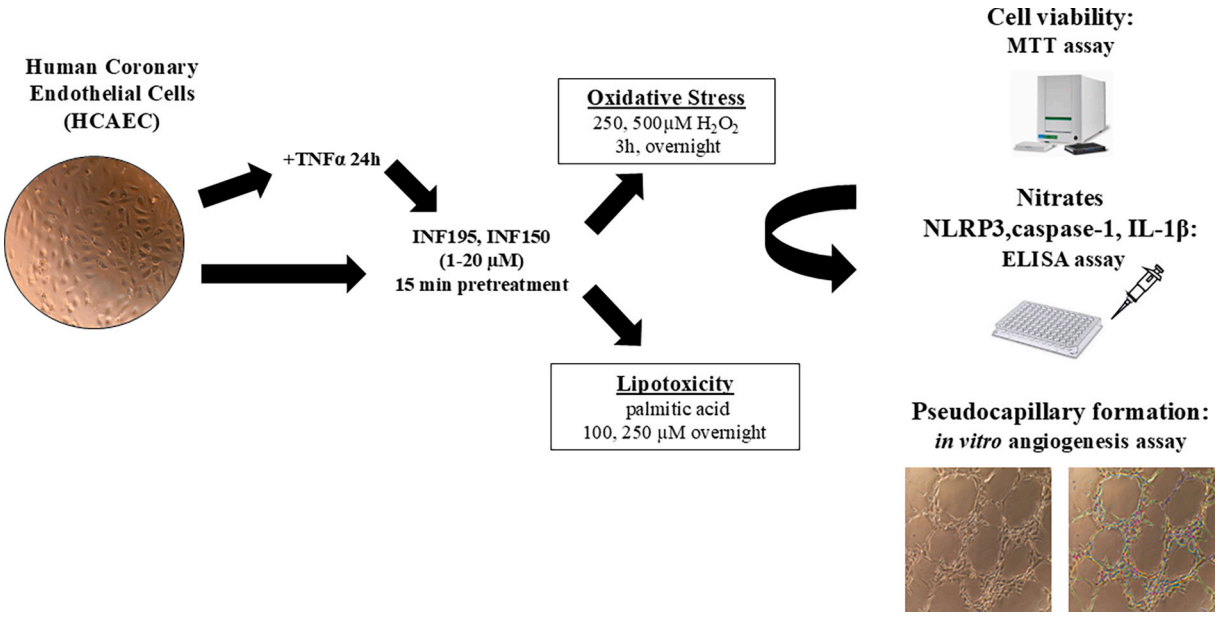



**Fig. 1. Experimental protocol**. HCAECs, either untreated or primed for 24 h with TNF-α, were treated with INF195 or INF150 for 15 min and subsequently stimulated with $H_2O_2$ or PA to induce oxidative stress or lipotoxicity. Then, cell viability, angiogenesis, IL-1β, and caspase-1 levels were measured.

## 1. Introduction

Endothelial dysfunction (ED) is a key early event in the pathogenesis of various cardiovascular diseases (CVDs), including atherosclerosis, heart failure, and ischaemia/reperfusion injury [1–3]. It is characterized by impaired endothelial responses to physiological stimuli. This dysfunction combined with upregulated pro-inflammatory state, predisposes the vasculature to a pro-atherogenic phenotype [4,5]. One of the major contributors to ED is oxidative stress, a condition caused by the excessive generation of reactive oxygen species (ROS), such as hydrogen peroxide ($H_2O_2$), exceeding the capacity of endogenous antioxidant defences [6]. This imbalance promotes inflammation and contributes to both microvascular and macrovascular injury.

Elevated levels of triglyceride-rich lipoproteins and lipid accumulation in non-adipose tissues are recognized risk factors for vascular inflammation and lipotoxicity. Particularly, in endothelial cells (ECs), which are poorly equipped to store lipids, high circulating levels of saturated free fatty acids (FFAs) lead to intracellular lipid overload and dysfunction [7]. FFAs strongly correlate with metabolic syndrome and are well-known contributors to CVDs [8]. Experimental evidence shows that FFAs induce the transcription of genes involved in oxidative stress and inflammation in ECs, increase ROS production, and exacerbate ED [9–11]. Palmitic acid (PA), one of the most abundant FFAs in human plasma, has been closely linked to lipotoxicity in diabetes [12]. It is also known to impair endothelial function through multiple mechanisms, including ROS generation and activation of the $Ca^{2+}$/protein kinase C-alpha/NADPH oxidase 4 (PKCα/NOX4) pathway [13].

The innate immune system represents the first line of defence against infections and cellular damage. Pattern recognition receptors (PRRs) detect pathogen-associated molecular patterns (PAMPs) and damage-associated molecular patterns (DAMPs), triggering inflammatory responses [14]. Among the PRRs, inflammasomes are cytosolic multiprotein complexes that mediate strong pro-inflammatory signalling. In particular, the NLRP3 (NOD-like receptor pyrin domain-containing 3) inflammasome is the most extensively studied and includes the sensor NLRP3, the adaptor ASC, and the effector caspase-1 [15,16]. The NACHT domain is a conserved nucleotide-binding and oligomerization domain essential for NLRP3 activation. It mediates ATP-dependent self-oligomerization, a critical step in inflammasome assembly and caspase-1 recruitment [17]. Upon activation, NLRP3 drives the autocatalytic activation of caspase-1, which in turn promotes the maturation and release of IL-1β and IL-18, as well as gasdermin D (GSDMD)-mediated pyroptosis [5]. Pyroptosis is a form of cell death involved in atherosclerosis [18] and endothelial cells are both targets and producers of IL-1β, amplifying inflammation through the release of secondary cytokines (e.g., IL-6 and C-reactive protein) and adhesion molecules [19].

Interestingly, ROS and FFAs can both function as DAMPs, activating the NLRP3 inflammasome and promoting endothelial inflammation and dysfunction. $H_2O_2$ activates the SIRT1/NF-κB/NLRP3 pathway in ECs, inducing pyroptosis [20]. Similarly, PA induces pyroptosis via NLRP3 activation in human umbilical vein endothelial cells (HUVECs) [21] and has been shown to contribute to ED *via* NLRP3-dependent mechanisms [22]. Overall, aberrant NLRP3 activation is increasingly recognized as a pathogenic factor in CVD [23,24].

Given the central role of NLRP3 in promoting low-grade inflammation, ED and CVD, we developed a novel series of small-molecule inhibitors targeting its NACHT domain, aiming to stabilize the inactive conformation of the complex [25,26]. Among these, INF195 and its active metabolite INF150 exhibit distinct cell-penetrating properties and differential cardioprotective and anti-inflammatory effects in both *in vitro* and *ex vivo* models [26,27]. Notably, INF150 is efficiently taken up by macrophages but shows limited penetration in cardiomyocytes, whereas INF195 is active in both cell types. Since ECs share features with both immune and parenchymal cells [28], we hypothesized that their capacity to internalize INF150 may be intermediate. Therefore, we investigated the ability of INF195 and INF150 to counteract oxidative stress and lipotoxicity in human coronary artery endothelial cells (HCAECs).

## 2. Materials and methods

### 2.1. Human endothelial cell cultures

Adult human coronary artery endothelial cells (HCAECs) and human umbilical vein endothelial cells (HUVECs) (ATCC, Manassas, VA, USA), were cultured in Endothelial Basal Medium supplemented with endothelial cell growth factors, following the manufacturer's instructions (Endothelial Cell Growth Kit-VEGF, ATCC, Manassas, VA, USA) and 5 % FBS (Euroclone, Milan, Italy), on gelatin-coated dishes (complete medium) [29]. Cells were grown in a humidified atmosphere with 5 % $CO_2$

in air, and the medium was refreshed every 2 days.

### 2.2. Experimental procedures

To assess the protective role of INF195 and INF150 on oxidative stress and lipotoxicity, HCAECs were pre-treated for 15 min with the inflammasome inhibitors and then stimulated with $H_2O_2$ (250 or 500 μM) or PA (100 or 250 μM) for 15–18 h (overnight). In some experiments, cells were primed with the inflammatory cytokine TNF-α (50 ng/mL) [30,31] for 24 h and then stimulated with PA (100 or 250 μM); this priming induces a heightened inflammatory state and increased stress responses in the cells (Fig. 1). In the pseudocapillary formation assay, HCAECs were treated for 3 h with $H_2O_2$ or with palmitate overnight, then cells were recovered and seeded on Geltrex™ for *in vitro* angiogenesis assay.

### 2.3. Bovine serum albumin (BSA)-Conjugated palmitate Preparation

Sodium palmitate (Sigma-Aldrich, St. Louis, MO, USA) was conjugated with bovine serum albumin (BSA, essentially fatty acid free; Sigma-Aldrich, St. Louis, MO, USA) to make a water-soluble fatty acid complex. First, 1.66 mM BSA in 150 mM NaCl was stirred at 37 °C. The sodium palmitate (PA) was solubilized in a BSA-$H_2O$ (1:1) solution and heated to 70 °C for 1 h [32].

### 2.4. Cell viability assay

MTT assay was employed to measure cellular metabolic activity as an indicator of cell vitality [26]. HCAECs were plated in 96-well culture plates (5.000 cells/well/100 μL) in complete EGM-2 medium. After 24 h complete medium was replaced with medium without growth factor and supplemented with 5 % FBS. Then, cells were treated with increasing concentrations (1, 10, 20 μM) of each compound in the presence of $H_2O_2$ (250 or 500 μM) or sodium palmitate (PA, 100 or 250 μM) overnight. MTT (at a final concentration of 5 mg/mL) was added to each well, followed by 4 h of incubation at 37 °C. Formazan crystals were dissolved by adding 150 μL of Isopropanol per well, followed by measurement of the absorbance at 570 nm by a microplate reader (Victor Nivo 2F, Revvity Italia SpA, Milan, Italy). BSA 0.1 % was chosen as a control for the highest PA concentration (20 μM).

### 2.5. Oil red O staining

Cellular lipid deposition was assessed by oil red O staining. HCAECs stimulated with 250 μM PA overnight were fixed with 4 % paraformaldehyde for 30 min. Cells were washed gently twice with $dH_2O$, and isopropanol (60 %) was added to each well and incubated for 5 min. Oil red O working solution was added and incubated for 10–20 min and then washed twice with $dH_2O$. Finally, cells were stained with hematoxylin, and pictures were taken under a bright field microscope.

### 2.6. Geltrex™ pseudo capillary formation

In vitro capillary morphogenesis was performed in tissue culture wells coated with Geltrex™ matrix (ThermoFisher Scientific, Milan, Italy) [33]. HCAECs were plated ($18 \times 10^3$/well) in EGM-2 medium without growth factors, supplemented with 2 % FBS and incubated at 37°C-5 % $CO_2$. Pictures were acquired at regular intervals with an EVOS optical microscope (Thermo Fisher Scientific, Monza, Italy). Results were quantified at 6 h using the Angiogenesis Analyzer in ImageJ (v1.9), followed by statistical analysis of each experimental condition. "Nodes" are identified as pixels that have at least three neighbours, corresponding to a bifurcation. "Junctions" are elements composed of several nodes. "Segments" are elements delimited by two junctions. "Meshes" are the polygon structures reinforced with more than one layer of cells in their walls and have also been referred to by other authors as a 'Honeycomb formation'. Six to nine photographic fields from three plates were scanned for each point.

### 2.7. ELISA assays

Caspase-1, NLRP3, and IL-1β levels were measured by ELISA assays. Briefly, HCAECs were plated in 6-well culture plates (40.000 cells/well/1 mL) in complete medium and allowed to grow until they reached 80 % confluence. Then cells were pre-treated with INF195 and INF150 for 15 min following PA for 24 h or $H_2O_2$ for 6 and 24 h. Media were collected, clarified by centrifugation at 14,000 rpm for 10 min at 4 °C, and supernatants were stored at − 80 °C. NLRP3, caspase-1 and IL-1β were measured by ELISA assays (FineTest, Wuhan, 430074, Hubei, China) according to the manufacturer's instructions.

### 2.8. Cytotoxicity assay

The pyroptotic cell death was evaluated after PA and $H_2O_2$ stimulation by measuring the lactate dehydrogenase (LDH) released in the cell supernatants according to the published procedure (Cytotoxicity detection kit, Roche Diagnostics GmbH, Mannheim Germany) [25]. In total, 50 μL of supernatants were added to a 96-well flat-bottom plate in triplicate samples. Then, 50 μL of reaction mixture was added to each well, and the plate was incubated for 30 min in the dark at room temperature. Following incubation, 50 μL of the supplied stop solution was added to each well. Optical density values were determined by measuring the absorbance at 492 nm using a plate-reading (Victor Nivo 2F, Revvity Italia SpA, Milan, Italy).

### 2.9. Nitrates levels

HCAECs were stimulated for 6 h with 100 μM PA or 250 μM $H_2O_2$, then supernatants were recovered, clarified by centrifugation at 14,000 rpm for 10 min at 4 °C and stored at − 80 °C. Nitrates were measured by nitric oxide (NO2/NO3) detection kit (Enzo Life Science, cat # ADI-917–010).

### 2.10. Western blot analysis

After harvesting the cells, the samples were resuspended in RIPA buffer (20 mM, pH 7.4) (Merk Millipore, Vimodrone, MI, Italy) containing proteinase inhibitors (Calbiochem, Merck, Darmstadt, Germany). After centrifugation at 14000 rpm for 7 min at 4° C, the supernatants were collected. Equal amounts of protein (30 μg), diluter in Laemmli buffer, were separated on Bolt® Bis-Tris Plus gels 4–12 % precast polyacrylamide gels (Biorad Laboratories, Italy) and transferred as previously reported [33]. Blots were blocked for 1 h at room temperature with 5 % milk in PBS 0.1 % containing Tween-20. Then, membranes were incubated overnight at 4 °C with the following primary antibodies: rabbit anti-gasdermin D (total and cleaved), L60 and (E5O4N) (1:1000, Cell Signaling Technology Leiden The Netherlands, cat#69469), and mouse anti-human HSP90 (sc-69703, 1:1000, Santa Cruz Biotecnology, Heidelberg, Germany). Subsequently, membranes were incubated with anti-rabbit IgG (whole molecule)–Peroxidase antibody (1:1000, Cat#7076S) or anti-mouse IgG (whole molecule)–peroxidase antibody (1:1000, Cat#7074S, Cell Signaling Technology, Leiden The Netherlands) as secondary antibodies. Protein bands were visualized using an enhanced chemiluminescence (ECL) detection system.

### 2.11. Statistical analysis

Statistical analysis was performed using GraphPad Prism 8.00 (GraphPad Software, San Diego, CA, USA). Parametric data were reported as Means ± SEM, and differences between groups were tested with the ANOVA test (followed by Bonferroni's and Dunnett's Multiple

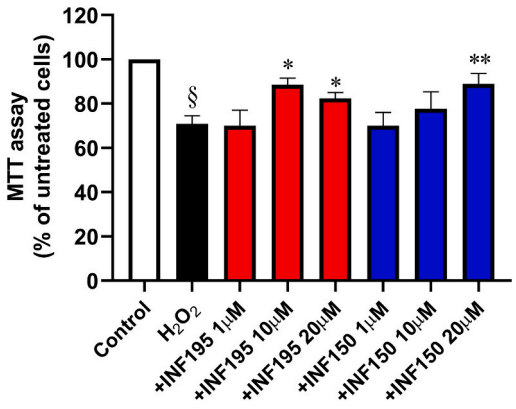



**Fig. 2. Cell viability in response to oxidative stress**. HCAECs were stimulated overnight with 250 μM $H_2O_2$ in the presence or absence of either INF195 or INF150, each tested at three separate concentrations. Results are expressed as mean ± SEM (n = 7). $^{§}P < 0.05$ vs control (untreated cells); *P < 0.05 ** P < 0.01 vs $H_2O_2$.

Comparison Test). For comparisons between two groups, Student's unpaired *t*-test was applied. The alpha value was set at 0.05.

## 3. Results

### *3.1. INF195 is more effective than INF150 in protecting against oxidative stress-induced cytotoxicity and palmitate-induced lipotoxicity*

To investigate whether inflammasome inhibitors can protect HCAECs from $H_2O_2$-induced oxidative stress, cells were stimulated overnight with 250 μM $H_2O_2$ in the presence of increasing concentrations of inflammasome inhibitors, ranging from 1 to 20 μM. Exposure to $H_2O_2$ significantly reduced HCAEC viability by 29.1 ± 3.7 % compared to untreated controls (Fig. 2). The addition of NLRP3 inhibitors significantly protected HCAECs from $H_2O_2$-induced damage, with INF195 being more effective than INF150. Notably, INF195 was protective at a concentration of 10 μM, restoring cell viability to 88.6 ± 2.9 % (vs. 70.8 ± 3.7 % with 250 μM $H_2O_2$ alone). At the same time, INF150 protected HCAECs only at the highest concentration, 20 μM, by restoring cell vitality to 88.8 ± 4.6 % (Fig. 2).

Higher $H_2O_2$ concentration (500 μM) showed similar results: cell viability was 43 ± 5 % and 60 ± 5 % in the absence and presence of 10 μM INF195 ($P < 0.05$ vs $H_2O_2$ alone), respectively, while 10 μM INF150 was less effective. At the highest concentration (20 μM), the two inhibitors were well tolerated and did not affect cell viability, as demonstrated by trypan blue exclusion observations (data not shown).

Since saturated fatty acid PA induces endothelial dysfunction, the effects of inflammasome inhibitors were assessed on PA-induced lipotoxicity. HCAECs were stimulated overnight with 250 μM PA, then lipid droplets were stained with Oil Red O. As shown in Fig. 3A, PA treatment significantly increased lipid droplets in HCAECs compared with the untreated cells, indicating lipid loading. This lipotoxicity reduced cell viability by 44.6 ± 7.3 % (Fig. 3B). When the endothelium was pre-treated with different concentrations of INF195, the percentage of viable cells significantly increased, starting from 1 μM (79.2 ± 3.8 %) and reaching a maximal effect at 10 μM (83.8 ± 8 %). INF150 protected cells only at the highest concentration, 20 μM, which restored cell viability to 80.5 ± 2.6 % (Fig. 3B). BSA (0.25 %), corresponding to 250 μM PA, did not modify cell viability (data not shown).

A lower PA concentration (100 μM) still induced lipotoxicity, resulting in a decrease of cell viability by 24.9 ± 4.7 %. Consistently, INF195 was able to counteract lipotoxicity with maximal effect at 1 μM, while INF150 protected endothelial cells only at the highest concentration used (20 μM) (Fig. 3C).

Since redox stress may be counteracted by nitric oxide (NO) [34], we measured nitrate levels as an index of NO availability. Both $H_2O_2$ and PA reduced nitrate levels, whereas treatment with INF195, at protective concentrations (Figs. 2 and 3), restored nitrate levels to values comparable to controls (Fig. 4). In contrast, INF150 did not restore nitrate

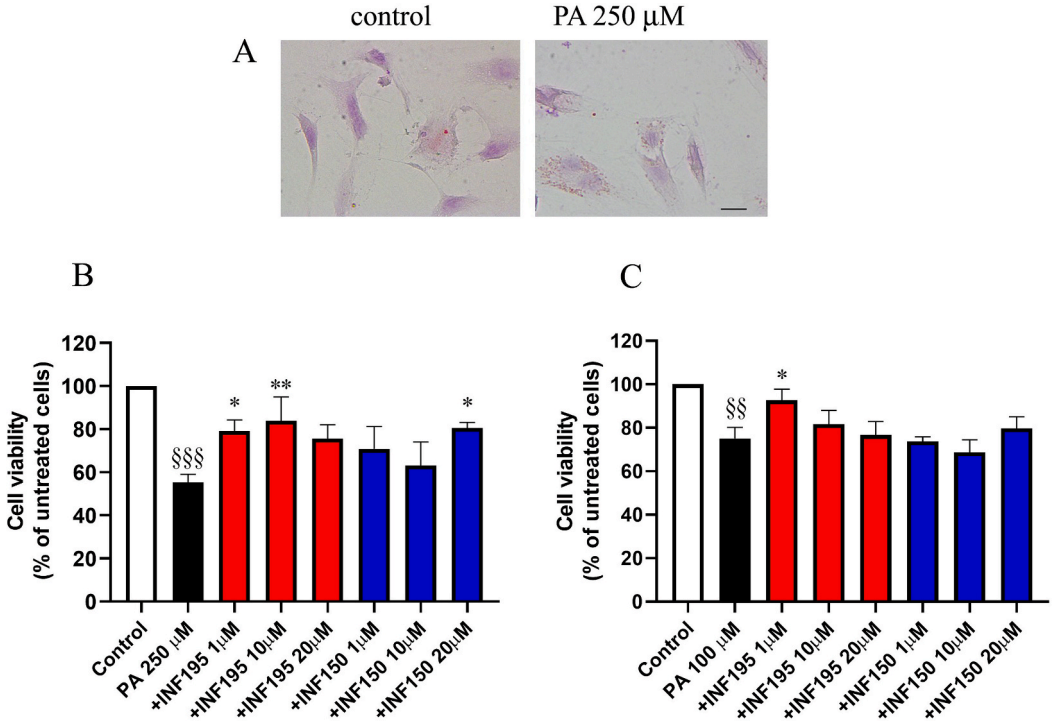



**Fig. 3. Cell viability in response to lipotoxicity**. HCAECs were stimulated overnight with 250 μM (A, B) or 100 μM PA (C) in the presence or absence of either INF195 or INF150. A) Intracellular lipid deposition was observed using oil red O (orange-red, scale bar: 20 μm). Results are expressed as mean ± SEM (n = 7). $^{§§§}P < 0.001$, $^{§§}P < 0.01$, vs control (untreated cells); *P < 0,05 **P < 0,01 vs PA.

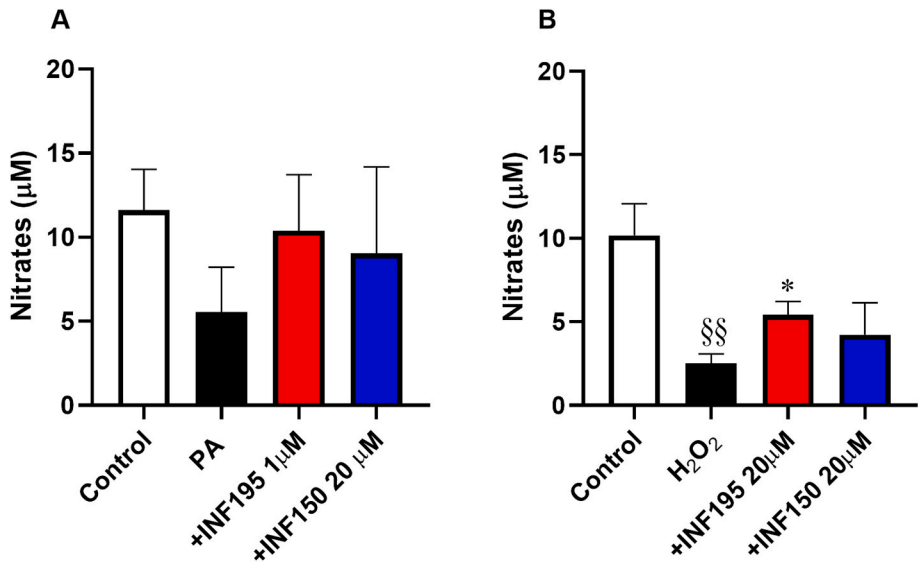



**Fig. 4.** Effect of **Nitrates levels**. HCAECs were stimulated for 6 h with 100 μM PA (**A**) or 250 μM $H_2O_2$ (**B**) in the presence of NLRP3 inhibitors, then nitrates levels were measured in the supernatants. Results are expressed as mean ± SEM (n = 3). $^{§§}P < 0.01$ vs control untreated cells; *<P0.05 vs $H_2O_2$.

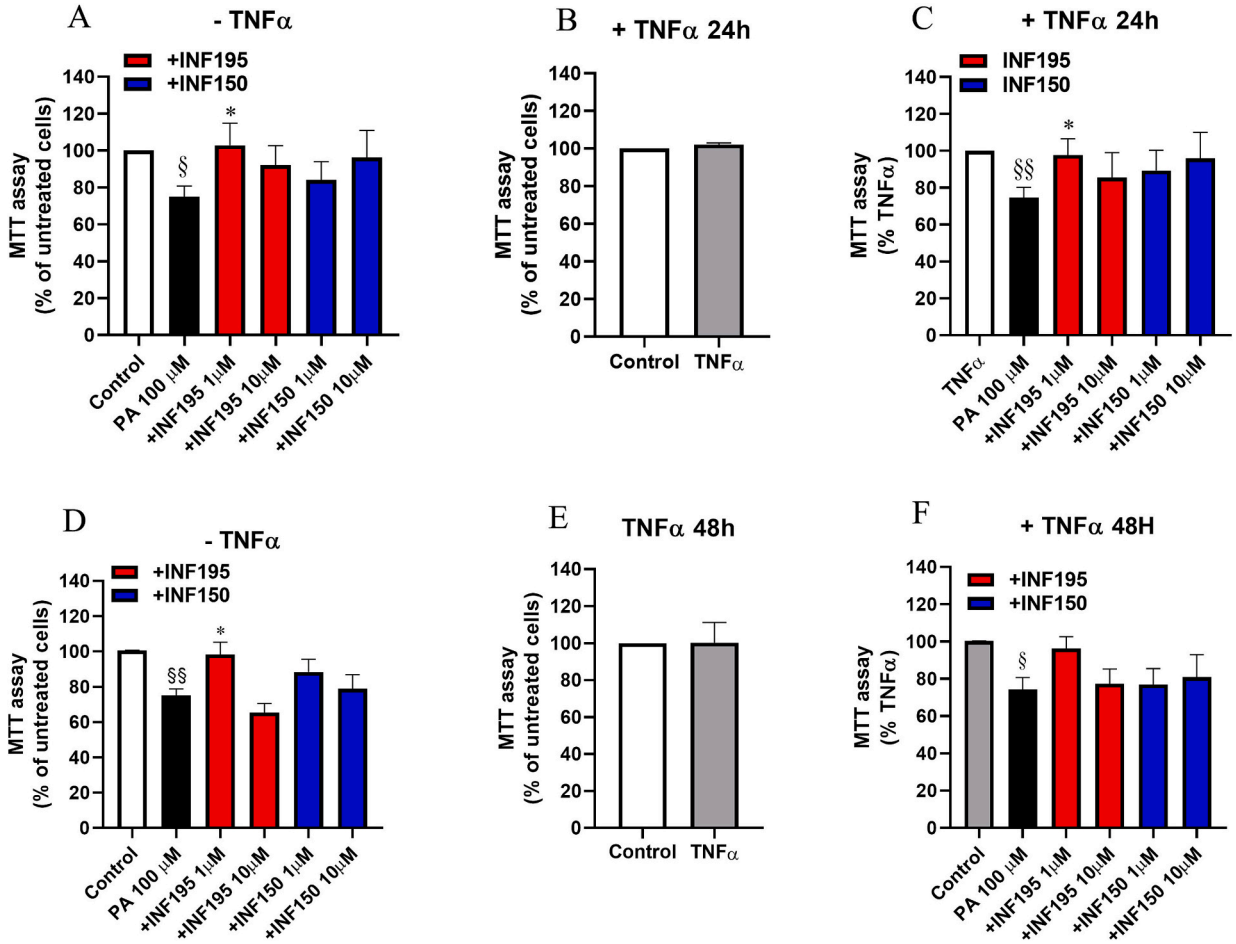



**Fig. 5. Effect of inflammasome inhibitors on TNF-α + PA-induced endothelial stress**. MTT assay. HCAECs without (**A, D**) or with a 24-h (**B, C**) or 48-h (**E, F**) priming with 50 ng/ml TNF-α, were stimulated overnight with 100 μM PA in the presence or absence of NLRP3 inhibitors. Mean ± SEM, n = 5. $^{§}P < 0.05$, vs control untreated cells; $^{§§}P < 0.01$vs TNF-α alone; *P < 0.05 vs PA.

levels to the same extent as INF195 (Fig. 4). These findings suggest that the protective effect of INF195 may involve nitric oxide-mediated mechanisms, an effect not observed with INF150.

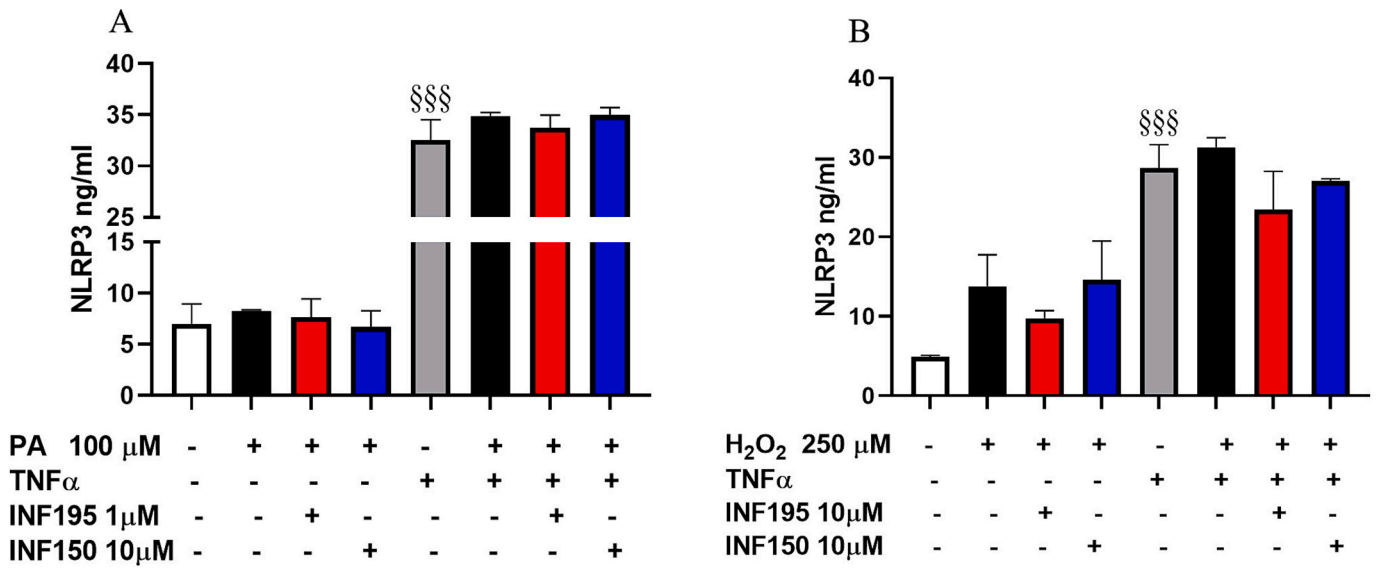



**Fig. 6. NLRP3 expression in HCAECs**. HCAECs were untreated or pretreated for 24 h with TNF-α, then stimulated with 100 μM PA (**A**) or 250 μM $H_2O_2$ (**B**), in the absence or presence of INF195 or INF150. Media were recovered, clarified, and used to measure NLRP3 expression by ELISA assay. Mean ± SEM, n = 3. $^{§§§}P < 0.001$ vs control (untreated cells).

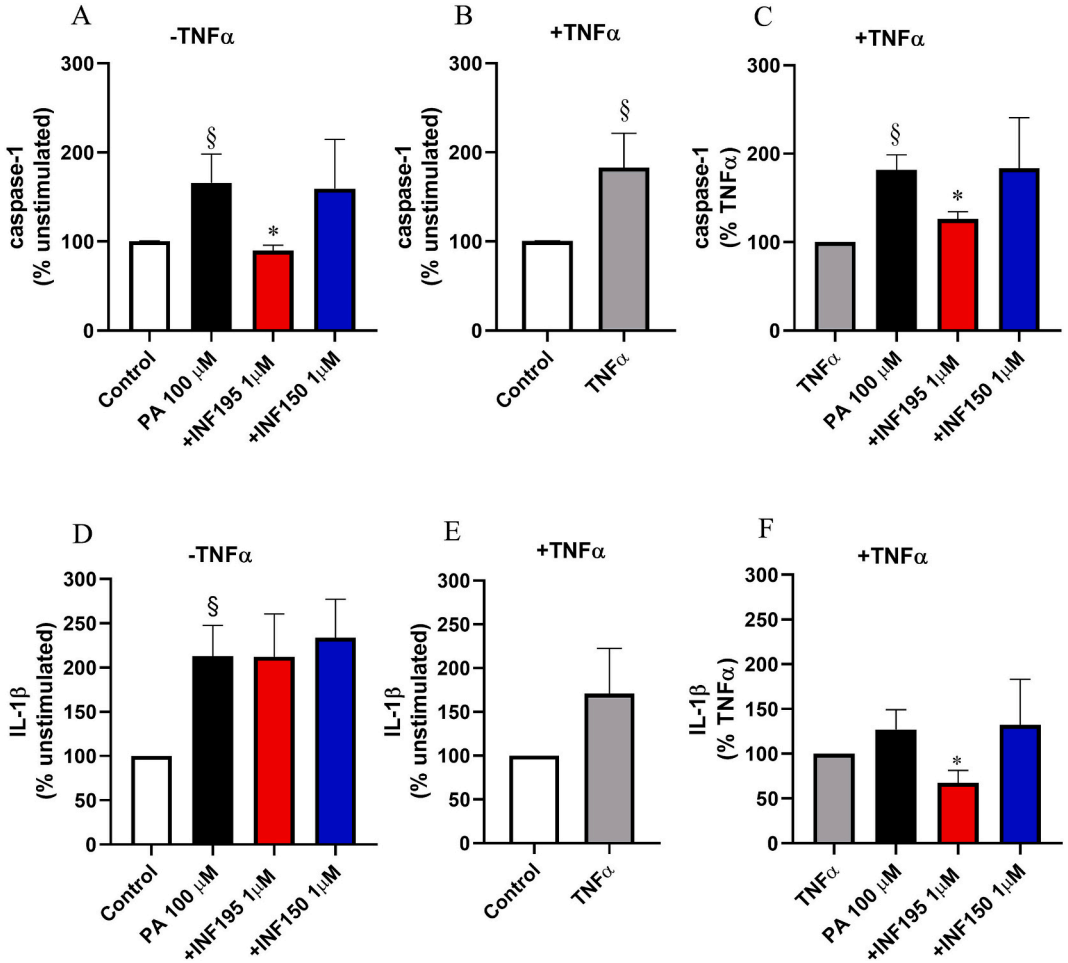



**Fig. 7. Levels of caspase-1 (A-C) and IL-1β release (D-F).** HCAECs were untreated (A, D) or pretreated for 24 h with TNF-α (B-C, E-F), then stimulated with 100 μM PA, in the absence or presence of INF195 and INF150. Media were recovered, clarified, and used to measure caspase-1 and IL-1β levels by ELISA assay. Mean ± SEM, n = 3. $^{§}P < 0.05$ vs control (untreated cells) (A-B, D-E,) or TNF-α (C, F); $^{*}P < 0.05$ vs PA.

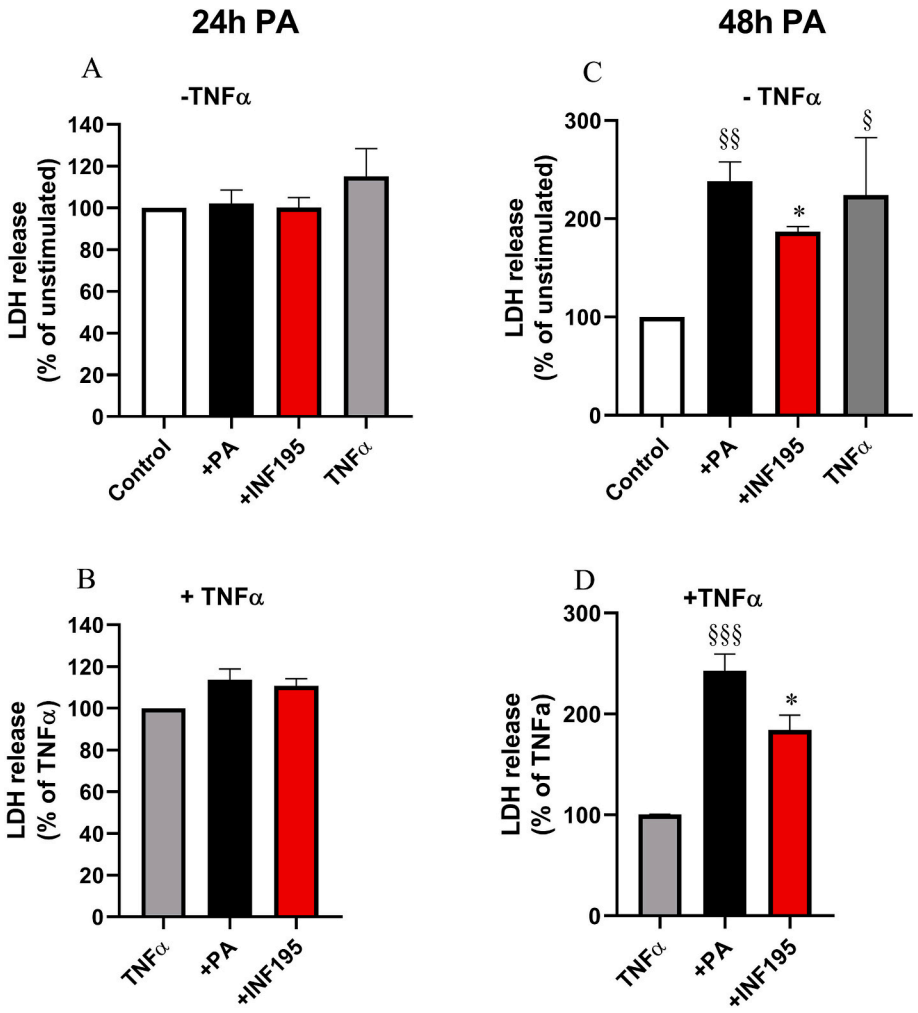



**Fig. 8. LDH release**. HCAECs without (**A, C**) and with a-24 h priming with TNF-α (**B, D**) were stimulated with 100 μM PA for 24 h (**A, B**) or 48 h (**C, D**) in the absence or presence of 1 μM INF195. Media were recovered, clarified, and used to measure LDH release, which is reported as % of control unstimulated cells, in the absence of TNF-α priming (**A, C**), and as % of TNF-α treated cells (used as control) (**B, D**). Mean ± SEM, n = 4. $^{§}P < 0.05$, $^{§§}P < 0.01$ vs control untreated; $^{§§§}P < 0.001$ vs TNF-α alone; *P < 0.05 vs PA.

### *3.2. INF195 protects endothelial cells primed with TNF-α and stimulated with PA*

The potential protective effects of INF195 and INF150 were also evaluated in an experimental condition that increased endothelial dysfunction. HCAECs were primed for 24 h with the inflammatory cytokine TNF-α (50 ng/mL) [30,31] and then stimulated overnight with 100 μM PA to assess cell viability in the presence or absence of inflammasome inhibitors, at the concentration most effective against PA and $H_2O_2$-induced effects. PA reduced HCAEC viability by approximately 25 %, and this effect was significantly prevented by INF195 1 μM (Fig. 5A), while INF150 at the same concentration was less effective. TNF-α priming alone did not affect cell viability (Fig. 5B), but it enhanced the cytotoxic effect of PA. Cell viability resulted in 75.9 ± 4 % without TNF-α priming and 69 ± 4 % with TNF-α priming (Fig. 5C). Again, INF195 was more effective than INF150 in protecting endothelial cells from the two inflammatory stimuli, with the maximal effect observed at the lowest concentration (1 μM, Fig. 5C). Similar results were obtained following 48 h-priming with TNF-α, where a protective trend was also observed with INF195 ($P < 0.060$, Student's T test, Fig. 5F).

### *3.3. The protective effect of INF195 is linked to NLRP3 inhibition without affecting its expression*

NLRP3 expression was significantly increased after cell priming with TNF-α and stimulation with PA or $H_2O_2$, and this enhanced expression was unaffected by INF195 or INF150 (Fig. 6). These data suggest that the protective effect of INF195 involves inhibition of NLRP3 activity rather than changes in its expression.

### *3.4. INF195 reduces downstream signalling of the NLRP3 inflammasome*

Lipotoxicity and oxidative stress lead to NLRP3 inflammasome assembly, caspase-1 activation, and cleavage of pro-IL-1β into mature IL-1β [35]. We assessed the levels of caspase-1 and IL-1β in the medium of endothelial cells, either untreated or treated with NLRP3 inhibitors (1 μM), following stimulation with PA (100 μM). The priming with TNF-α (50 ng/ml, 24 h) was also investigated. PA significantly increased caspase-1 levels, and INF195 significantly prevented this increase, while INF150 at the same concentration was ineffective (Fig. 7A). Additionally, 24 h-priming of cells with TNF-α significantly enhanced caspase-1 level (Fig. 7B), which was further increased by PA, and was significantly inhibited by 1 μM INF195 (Fig. 7C). INF150 did not counteract the increase of caspase-1 in response to PA (Fig. 7C).

We next measured IL-1β levels as a downstream consequence of

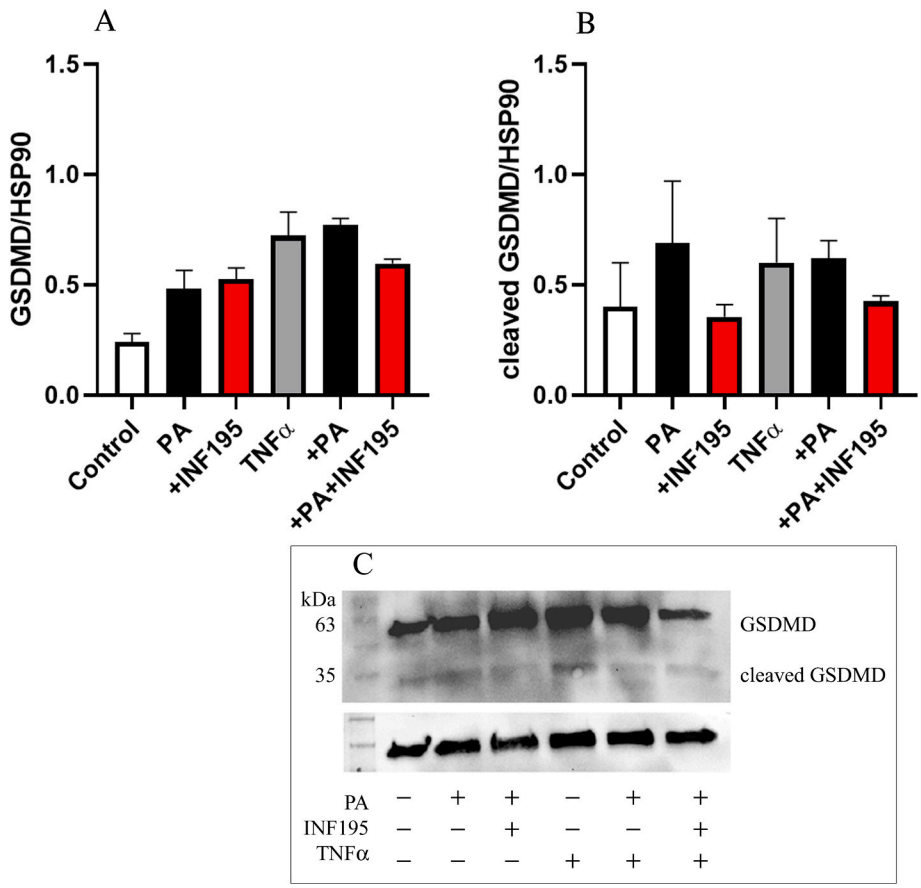



**Fig. 9. Western blot analysis for Gasdermin D expression**. HCAEC without and with a-24 h priming with TNF-α were stimulated with 100 μM PA for 48 h in the absence or presence of 1 μM INF195. Cell lysates were used to perform Western blot analysis for evaluating total (A) and cleaved (B) gasdermin D expression. Mean ± SEM, n = 3. C) Representative experiment.

caspase-1 activation. Exposure to high PA concentration (250 μM) for 24 h increased IL-1β levels, an effect that was significantly inhibited by 1 μM INF195. Baseline IL-1β concentration was 23 ± 1.4 pg/ml, which increased to 33 ± 4 pg/ml in response to PA and returned to basal levels in the presence of INF195 (21.7 ± 1.08 pg/ml).

We then stimulated HCAECs with a lower concentration of PA (100 μM) with or without 24 h TNF-α priming. INF195 did not prevent IL-1β release induced by a low PA concentration in the absence of the TNF-α priming (Fig. 7D). Instead, TNF-α priming enhanced IL-1β levels to 185 ± 50 % vs unstimulated (Fig. 7E), and 1 μM INF195 significantly reduced IL-1β levels in response to the combined TNF-α + PA treatment, decreasing the response induced by TNF-α by 33 ± 10 % (Fig. 7F). IL-1β levels elevated by PA were not reduced by the same concentration of INF150 (Fig. 7F).

### 3.5. *INF195 inhibits NLRP3-induced endothelial cell pyroptosis*

Since LDH is released during pyroptosis [36], we assessed the LDH release in response to 100 μM PA stimulation, with or without the TNF-α priming. As expected, 100 μM PA for 24 h did not induce pyroptosis, since it did not significantly enhance LDH release (Fig. 8A). Also, the 24 h-priming of cells with TNF-α did not increase LDH release (Fig. 8B), in agreement with MTT data (Fig. 5B), suggesting a decrease in cell function without complete cell death. An increase in LDH production was observed when endothelial cells were stimulated for 48 h with 100 μM PA, which consistently decreased cell viability, with an enhanced LDH release, suggesting cell pyroptosis (Fig. 8C). INF195 was able to inhibit pyroptosis even in cells exposed to both TNF-α priming and PA stimulation for 48 h (Fig. 8D). The expression of cleaved gasdermin D confirmed the occurrence of cell pyroptosis after 48 h of PA stimulation, particularly in TNF-α primed cells, and INF195 reduced gasdermin D activation (Fig. 9).

### 3.6. *INF195 and INF150 differentially protect HCAECs and HUVECs from angiogenic dysfunction induced by oxidative and lipotoxic stress*

Based on data showing that inflammasome inhibitors protect the endothelial cells from established stressors, we aimed to assess the potential protective effect of the most effective inhibitor, INF195, on the impairment of endothelial function induced by low concentrations of PA and $H_2O_2$. We aimed to promote endothelial dysfunction, without causing cell death. Cultured endothelial cells were pretreated with INF195 for 15 min, then exposed either to 250 μM $H_2O_2$ for 3 h or to 100 μM PA overnight. Following treatment, cells were harvested from the culture dish and seeded on Geltrex™ to assess their angiogenic potential. Within 6 h, the endothelium organized itself into tubular structures. Although the 3-hour treatment with $H_2O_2$ did not induce cell death (Fig. 10A), it impaired functional behaviour, since cells could not form pseudocapillaries (Fig. 10B). $H_2O_2$ promoted a significant reduction in the number of nodes, master junctions, master segment length, and total segment length (Fig. 9C). Moreover, endothelial cells displayed a stressed morphology (Fig. 10B). INF195 (10 μM) significantly restored endothelial cell ability to form *in vitro* preucocapillaries (Fig. 10C).

The effect of INF195 was also assessed on PA-induced angiogenesis impairment. HCAECs were pretreated with INF195 (10 μM) for 15 min, stimulated overnight with the lowest PA concentration (100 μM), then were recovered to evaluate pseudocapillaries formation. PA reduced the pseudocapillary network by HCAECs, as evidenced by the formation of

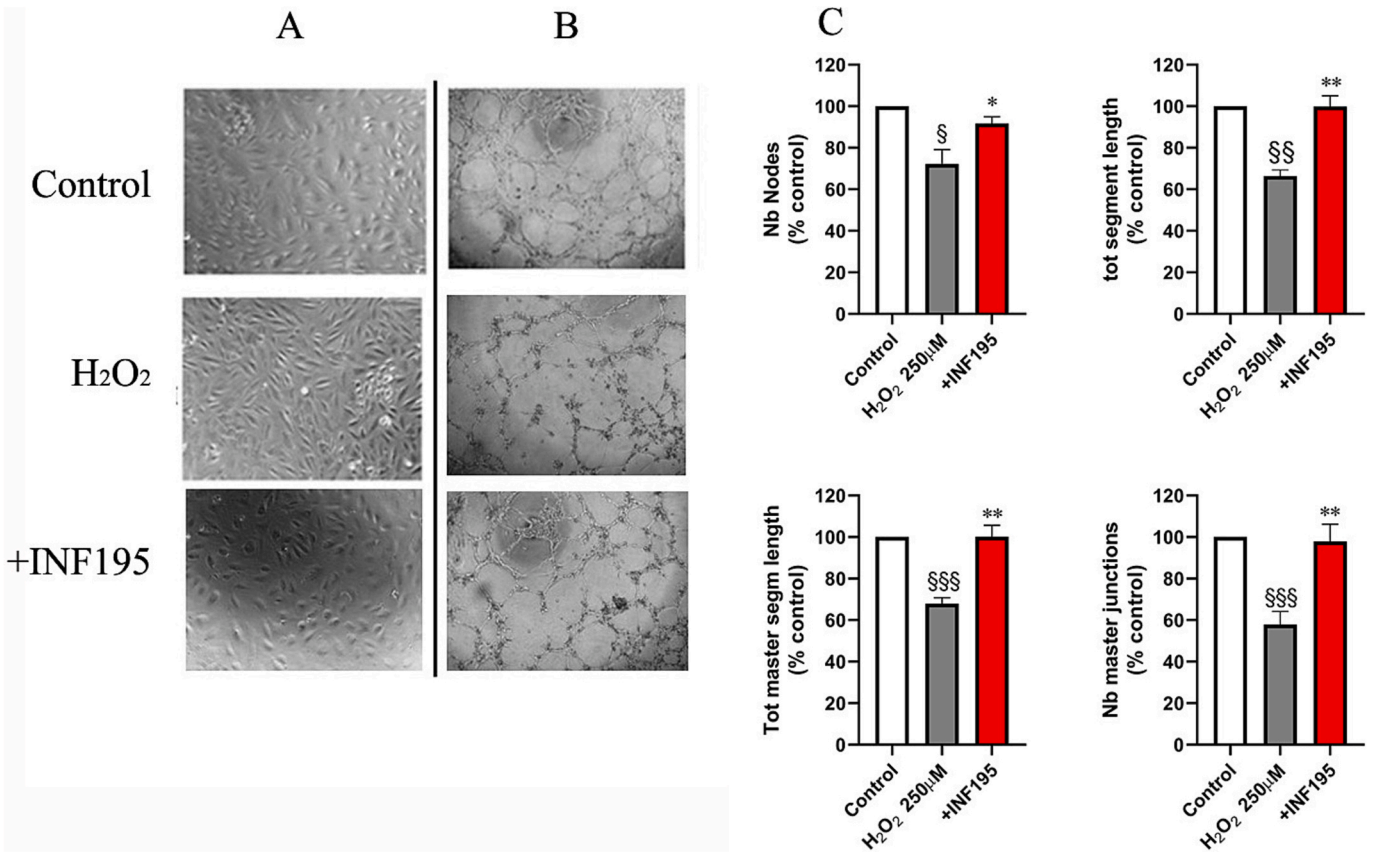



**Fig. 10. Effect of INF195 on angiogenesis damage induced by oxidative stress.** Cultured HCAECs were pretreated for 15 min with 10 µM INF195, stimulated for 3 h with 250 µM $H_2O_2$ (**A**, representative pictures), then recovered from the dishes and seeded on Geltrex™ matrix. After 6 h, the pseudocapillaries formed were observed under a light microscope (4X magnification) and photographed (**B**, representative pictures). **C**) Images were analyzed with the Image J program to quantify angiogenesis, as the number of nodes, master junctions, master segment length, and total segment length. Data are expressed as a percentage of untreated cells (control). Mean ± SEM n = 3. $^{\S}P < 0.05$, $^{\S\S}P < 0.01$ $^{\S\S\S}P < 0.001$ vs control (untreated cells); $^{*}P < 0.05$, $^{**}P < 0.01$ vs $H_2O_2$.

fewer tubular structures (Fig. 11B). INF195 significantly inhibited PA-induced damage by increasing the number of junctions, segments, total master segment length, and total segment length (Fig. 11A).

The protective effect of INF195 was confirmed in HUVECs, which are widely used and historically regarded as the gold standard for *in vitro* angiogenesis assays. HUVEC viability decreased by 16 ± 4 % and 46.9 ± 3.0 % in response to 100 µM and 250 µM PA, respectively (Fig. 12 A, B). INF195 counteracted PA effects with maximal protection obtained with the concentration of 1 µM, which completely prevented cell damage. INF150 protected cells only at the highest concentration, 20 µM, which completely prevented cell injury in response to 100 µM PA and restored cell viability to 78.2 ± 5.6 % when cells were treated with 250 µM PA (Fig. 12 A, B).

INF195 also protected endothelial cells from $H_2O_2$-induced oxidative stress, with the lowest concentration (1 µM) being the most effective, as it completely prevented cell damage (Fig. 12 C, D). Once again, INF195 significantly prevented angiogenic damage even when HUVECs showed a severely compromised ability to form tubular structures in response to high $H_2O_2$ concentrations (500 µM). $H_2O_2$ reduced the number of junctions by 72 ± 5.3 % of control levels, whereas the INF195 treatment restored this parameter to 58 ± 8 % (42 % reduction of the unstimulated control, $P < 0.05$). Similarly, the number of nodes decreased by 73 ± 5 % following 500 µM $H_2O_2$ exposure and was restored to 55 ± 9 % by INF195 ($P < 0.01$). At lower $H_2O_2$ concentrations (250 µM) the protective effect of INF195 was complete (Fig. 12E). Likewise, exposure of HUVECs to 100 µM PA significantly impaired the angiogenesis process, reducing it by approximately 25–30 % of control levels. INF195 almost completely protected the endothelium from this injury (Fig. 12F).

## 4. Discussion

In the present study, we compared the efficacy of INF195 and its active metabolite INF150 in different models of endothelial dysfunction. We found that INF195 exhibits greater efficacy than INF150 in protecting HCAECs against oxidative stress and lipotoxicity. While INF150 shows some protective effects, these are only evident at higher concentrations, suggesting a reduced ability to penetrate endothelial cells compared to INF195. This observation aligns with previous findings indicating that INF150 is efficiently taken up by macrophages but does not penetrate cardiomyocytes, whereas INF195 is active in both cell types at low concentrations [26,27]. Given that HCAECs share features with both immune and parenchymal cells [28], our results support the idea of an intermediate capacity for INF150 uptake, which may explain its lower efficacy in this cell type.

Oxidative stress and lipotoxicity are highly responsible for endothelial dysfunction. They are recognized as DAMPs leading to NLRP3 activation, exacerbating endothelial dysfunction and promoting CVD [12,37]. The pivotal role of the inflammasome in CVD is also demonstrated by the beneficial effects of statins, and other anti-inflammatory or antioxidant drugs on vascular dysfunction, by inhibiting NLRP3 inflammasome pathway [38–40]. Recently, liraglutide has been demonstrated to mitigate apoptosis of HUVECs induced by high glucose, oxidative stress and inflammasome activation *via* regulating the TRIB3/NF-κB/IκB-α signaling pathway [41], corroborating the role of the NLRP3 pathway in endothelial dysfunction.

In our study, we demonstrate that INF195 significantly protects HCAECs against oxidative stress and lipotoxicity. INF195 enhances HCAEC survival exposed to $H_2O_2$ and PA. Most notably, INF195

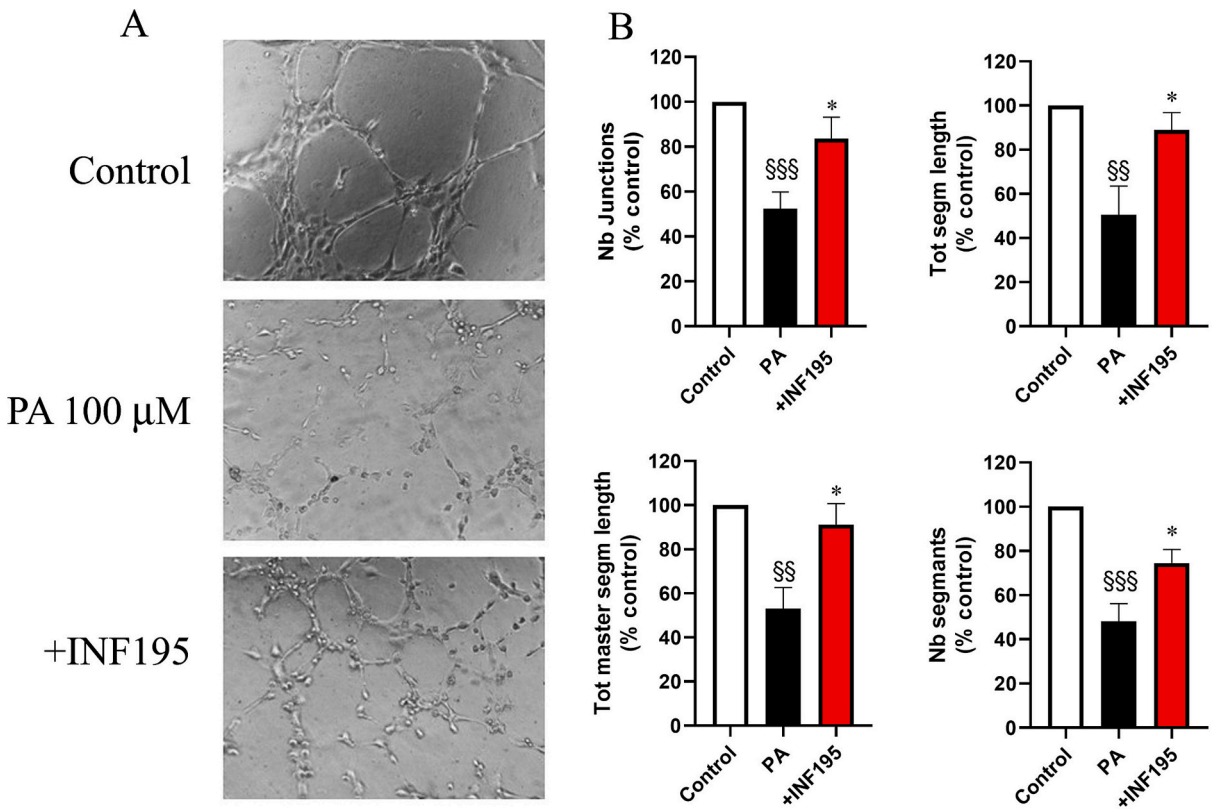



**Fig. 11. Effect of INF195 on angiogenesis injury induced by lipotoxicity**. HCAECs were pretreated for 15 min with 10 μM INF195, stimulated with 100 μM PA overnight, recovered from the plate and seeded on GeltrexTM matrix. After 6 h, the pseudocapillaries formed were observed under a light microscope (4X magnification) and photographed. A) Representative pictures (10x). B) The images were analyzed with the Image J program to quantify angiogenesis, as the number of junctions, segments, total master segment length and total segment length. Data are expressed as a percentage of untreated cells (control). Mean ± SEM n = 5. $^{§§}P < 0.01$ $^{§§§}P < 0.001$ vs control (untreated cells); $^{*}P < 0.05$, vs PA.

significantly reduces the detrimental effects of $H_2O_2$ and PA on *in vitro* pseudocapillary formation. The protective effect of INF195 is, at least in part, attributable to nitric oxide production, as suggested by restored nitrate levels after NLRP3 inhibition.

NLRP3 was previously reported to be activated in human endothelial cells in response to oxidative stress and FFA. FFA was reported to activate NLRP3 inflammasome in HUVECs and induce IL-1β release through AMP-activated protein kinase, both *in vitro* and in vivo on aorta of mice fed with a high-fat diet [22]. Liu and collaborators showed that high $H_2O_2$ concentrations up to 400 μM significantly increased intracellular ROS, which contributed to the induction of NLRP3 expression and pyroptosis. Through the downregulation of NLRP3 and the use of caspase-1 inhibitor VX-765, the occurrence of cell pyroptosis decreased [20]. We confirm that INF195 effectively inhibits NLRP3 activation and its downstream signaling, while also limiting pyroptosis.

Numerous studies have investigated the cardioprotective effects of direct NLRP3 inhibitors. However, limited data are reported on endothelial function. MCC950 has been shown to attenuate HUVEC senescence induced by the S protein of SARS-CoV2 [42]. Additionally, the inflammasome inhibitor INF39 significantly reduced monocyte and platelet adhesion to HUVEC as well as IL-1 overexpression in response to high glucose levels [43]. Some naturally derived substances have also demonstrated protective effects on HUVEC viability in response to oxidative stress and inflammation, possibly through NLRP3 inhibition. Procyanidin B2, a naturally occurring flavonoid found in dietary sources, exhibited robust inhibitory effects on NLRP3 inflammasome activation in rat lung tissue models and significantly suppressed the activation of NLRP3 inflammasome and caspase-1 activation in HUVECs [44]. Puerarin, an isoflavone derivative isolated from Pue, has been reported to protect from ischemia-reperfusion injury [45] and restored HUVECs from apoptosis and pyroptosis mediated by NLRP3 [46]. Our present study demonstrates, for the first time, that a direct NLRP3 inhibitor can protect human coronary artery endothelial cells from dysfunction induced by low PA and $H_2O_2$ concentrations, under conditions that did not cause cell death. We further evaluated the effect of INF195 on endothelial cells exposed to inflammatory stimuli, by priming HCAECs with TNF-α, followed by stimulation with low dose of PA. We demonstrate that short-term exposure to low concentration of PA does not induce pyroptosis, as evidenced by unmodified LDH release, but results in impaired cell function, suggesting the presence of endothelial cell dysfunction. Notably, IL1-β levels were reduced in the presence of INF195, supporting its anti-inflammatory effects.

An interesting finding is the effective concentration of INF195 in protecting human coronary endothelial cells. INF195 is active at micromolar concentrations, and lower concentrations are more effective than the higher ones, particularly when endothelial cells were exposed to a dual inflammatory stimulus. These findings are in line with previous studies, in which low doses of INF195 protected against myocardial ischemia/reperfusion injury in *ex vivo* mouse models [26]. This non-dose-dependent activity of INF195 is under investigation. It may reflect a dual role of this inhibitor or the activation of distinct pathways in response to higher INF195 concentrations [26].

INF150, the active metabolite of INF195, is less effective than INF195 in protecting endothelial cells. This result is in line with our previous one, where INF150 did not demonstrate cardioprotective effects in the *ex vivo* ischemia–reperfusion model, although it modulated macrophage function. An explanation can be the different permeability of this compound in cells. We demonstrated, indeed, that INF150 did not penetrate naïve and differentiated H9c2 cells, while it reduced NLRP3-driven pyroptosis and IL-1β release in a macrophage cellular model [26].

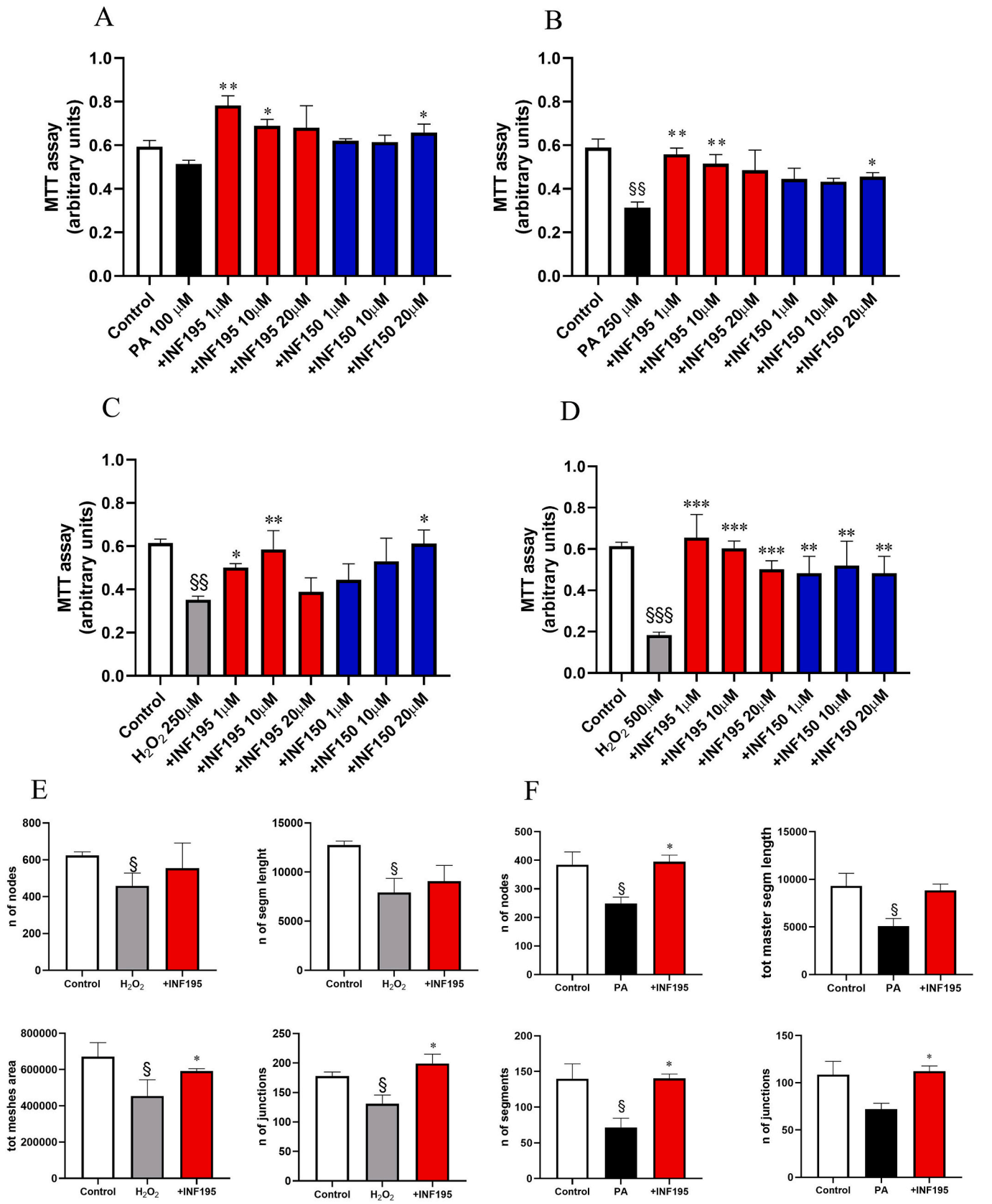



**Fig. 12. INF195 protected HUVECs from oxidative stress and lipotoxicity**. A-D) Cell viability in response to PA (100–250 μM) and H2O2 (250–500 μM). Mean ± SEM, n = 3. $^{§§}P < 00.1$, $^{§§§}P < 0.001$ vs control untreated cells; *P < 0.05, **P < 0.01, ***P < 0.001 vs PA or H2O2. E-F) Effect of INF195 on *in vitro* angiogenesis. HUVECs were stimulated for 3 h with 250 μM $H_2O_2$ (E) or 100 μM PA (F), then recovered from the plate and seeded onto a GektrexTM matrix. After 6 h, the pseudocapillaries formed were observed under a light microscope (4X magnification) and photographed. The images were analyzed with the Image J program to quantify angiogenesis. Mean ± SD n = 2. $^{§}P < 0.0$, $^{§§§}P < 0.001$ vs control (untreated cells) (control, C); *P < 0.05 **P < 0.01 vs $H_2O_2$ or PA.

Our present data demonstrate that INF195 restored the ability of HCAECs to form pseudocapillares, a process that was impaired by PA and $H_2O_2$. Notably, the exposure of cells to low PA and $H_2O_2$ concentrations did not induce cell death, as demonstrated by LDH release, but significantly impaired their capacity to form tubular structures. INF195 partially reduced this cellular impairment in HCAECs and also in HUVECs, considered the gold standard for *in vitro* angiogenesis assay.

Inflammasome inhibition by INF195 is confirmed by experiments showing reduced caspase-1 levels and decreased release of IL-1β, the latter being a marker of caspase-1 activity, in cells exposed to low concentrations of PA. Consistently, INF150 is unable to protect endothelial cells under the same conditions. Furthermore, exposure to high PA concentrations leads to a significant increase in LDH, suggesting pyroptosis. Notably, INF195 is able to partially, but significantly, counteract this effect.

### 4.1. Conclusions

In conclusion, our study demonstrates for the first time that the direct NLRP3 inhibitor INF195 provides significant protection to human coronary endothelial cells against oxidative and lipotoxic stress, preserving cell viability and angiogenic function, and limiting pyroptosis. These findings support the potential of INF195 as a therapeutic candidate for preventing or limiting endothelial dysfunction in cardiovascular diseases.

## CRediT authorship contribution statement

**Astrid Parenti:** Writing – review & editing, Writing – original draft, Validation, Supervision, Software, Methodology, Funding acquisition, Data curation, Conceptualization. **Costanza Titi:** Investigation. **Arianna Brovero:** Investigation. **Federica Blua:** Writing – review & editing, Validation, Methodology. **Francesca Boccato:** Validation, Methodology. **Angela Silvano:** Software, Investigation. **Francesco Fedele:** Visualization, Validation, Funding acquisition. **Anna Vittoria Mattioli:** Visualization, Validation. **Massimo Bertinaria:** Validation, Supervision, Methodology, Funding acquisition. **Pasquale Pagliaro:** Writing – review & editing, Visualization, Validation, Supervision, Funding acquisition. **Claudia Penna:** Writing – review & editing, Validation, Supervision, Funding acquisition, Formal analysis, Conceptualization.

## Declaration of competing interest

The authors declare that they have no known competing financial interests or personal relationships that could have appeared to influence the work reported in this paper.

## Acknowledgments

This work was supported by INRC (National Institute for Cardiovascular Research), Bologna, Italy: Donazione Anna Maria Ruvinetti; by grants from University of Florence (research funding) and Progetti PRIN: PAGP_PRIN_2022_23_01-2022AA37N3. BERM_PRIN_2022_23_02 - 20229WP2JJ. PENC_PRIN_2022_23_01-2022S74XWB. "Finanziato dall'Unione europea- Next Generation EU, Missione 4 Componente 1 CUP: D53D23013360006, D53D23012320006 and D53D23014490006".

## Data availability

The data that has been used is confidential.

## References

[1] H. Cai, D.G. Harrison, Endothelial dysfunction in cardiovascular diseases: the role of oxidant stress, Circ. Res. 87 (10) (2000) 840–844, https://doi.org/10.1161/01.res.87.10.840.
[2] A. Kibel, A.M. Lukinac, V. Dambic, I. Juric, K. Selthofer-Relatic, Oxidative stress in Ischemic Heart Disease, Oxid. Med. Cell. Longev. 2020 (2020) 6627144, https://doi.org/10.1155/2020/6627144.
[3] C. Penna, P. Pagliaro, Endothelial Dysfunction: Redox Imbalance, NLRP3 Inflammasome, and Inflammatory responses in Cardiovascular Diseases, Antioxidants (basel) 14 (3) (2025) 256, https://doi.org/10.3390/antiox14030256.
[4] R. Dhananjayan, K.S. Koundinya, T. Malati, V.K. Kutala, Endothelial Dysfunction in Type 2 Diabetes Mellitus, Indian J. Clin. Biochem. 31 (4) (2016) 372–379, https://doi.org/10.1007/s12291-015-0516-y.
[5] J. Wu, M. Shyy, J.Y. Shyy, H. Xiao, Role of inflammasomes in endothelial dysfunction, Br. J. Pharmacol. 181 (24) (2024) 4958–4972, https://doi.org/10.1111/bph.16479.
[6] B. Bai, Y. Yang, Q. Wang, M. Li, C. Tian, Y. Liu, L.H.H. Aung, P.F. Li, T. Yu, X. M. Chu, NLRP3 inflammasome in endothelial dysfunction, Cell Death Dis. 11 (2020) 776, https://doi.org/10.1038/s41419-020-02985-x.
[7] A. Karmi, P. Iozzo, A. Viljanen, J. Hirvonen, B.A. Fielding, K. Virtanen, V. Oikonen, J. Kemppainen, T. Viljanen, L. Guiducci, M. Haaparanta-Solin, K. Någren, O. Solin, P. Nuutila, Increased brain fatty acid uptake in metabolic syndrome, Diabetes 59 (9) (2010) 2171–2177, https://doi.org/10.2337/db09-0138.
[8] S. Qin, J. Yin, K. Huang, Free fatty acids increase intracellular lipid accumulation and oxidative stress by modulating PPARα and SREBP-1c in L-02 cells, Lipids 51 (7) (2016) 797–805, https://doi.org/10.1007/s11745-016-4160-y.
[9] T. Yuan, T. Yang, H. Chen, D. Fu, Y. Hu, J. Wang, Q. Yuan, H. Yu, W. Xu, X. Xie, New insights into oxidative stress and inflammation during diabetes mellitus-accelerated atherosclerosis, Redox Biol. 20 (2019) 247–260, https://doi.org/10.1016/j.redox.2018.09.025.
[10] R. Mallick, A.K. Duttaroy, Modulation of endothelium function by fatty acids, Mol. Cell. Biochem. 477 (1) (2022) 15–38, https://doi.org/10.1007/s11010-021-04260-9.
[11] M. Rhee, J. Lee, E.Y. Lee, K.H. Yoon, S.H. Lee, Lipid Variability Induces Endothelial Dysfunction by increasing Inflammation and Oxidative stress, Endocrinol Metab (seoul). 39 (3) (2024) 511–520, https://doi.org/10.3803/EnM.2023.1915.
[12] L. Ghosh, A. Gao, P.M. Thakur, C.W.K.L. Siu, Role of free fatty acids in endothelial dysfunction, J. Biomed. Sci. 24 (1) (2017) 50, https://doi.org/10.1186/s12929-017-0357-5.
[13] P. Chen, H. Liu, H. Xiang, J. Zhou, Z. Zeng, R. Chen, S. Zhao, J. Xiao, Z. Shu, S. Chen, H. Lu, Palmitic acid-induced autophagy increases reactive oxygen species via the Ca2+/PKCα/NOX4 pathway and impairs endothelial function in human umbilical vein endothelial cells, Exp. Ther. Med. 4 (2019) 2425–2432, https://doi.org/10.3892/etm.2019.7269.
[14] T. Gong, L. Liu, W. Jiang, R. Zhou, DAMP-sensing receptors in sterile inflammation and inflammatory diseases, Nat. Rev. Immunol. 20 (2) (2020) 95–112, https://doi.org/10.1038/s41577-019-0215-7.
[15] F. Martinon, K. Burns, J. Tschopp, The inflammasome: a molecular platform triggering activation of inflammatory caspases and processing of proIL-beta, Mol. Cell 10 (2) (2002) 417–426, https://doi.org/10.1016/s1097-2765(02)00599-3.
[16] M.S.J. Mangan, E.J. Olhava, W.R. Roush, H.M. Seidel, G.D. Glick, E. Latz, Targeting the NLRP3 inflammasome in inflammatory diseases, Nat. Rev. Drug Discov. 17 (8) (2018) 588–606. Erratum in: Nat. Rev. Drug Discov. 17 (9) (2018) 688. doi: 10.1038/nrd.2018.97.
[17] S. Paik, J.K. Kim, P. Silwal, C. Sasakawa, E.K. Jo, An update on the regulatory mechanisms of NLRP3 inflammasome activation, Cell. Mol. Immunol. 18 (5) (2021) 1141–1160, https://doi.org/10.1038/s41423-021-00670-3.
[18] X. He, X. Fan, B. Bai, N. Lu, S. Zhang, L. Zhang, Pyroptosis is a critical immune-inflammatory response involved in atherosclerosis, Pharmacol. Res. 165 (2021) 105447, https://doi.org/10.1016/j.phrs.2021.105447.
[19] A. Grebe, F. Hoss, E. Latz, NLRP3 inflammasome and the IL-1 pathway in atherosclerosis, Circ. Res. 122 (12) (2018) 1722–1740, https://doi.org/10.1161/CIRCRESAHA.118.311362.
[20] J. Liu, Y. Yan, D. Zheng, J. Zhang, J. Wang, Inhibiting microRNA-200a-3p attenuates pyroptosis via targeting the SIRT1/NF-κB/NLRP3 pathway in H2O2-induced HAEC, Aging (Albany NY) 15 (20) (2023) 11184–11200, https://doi.org/10.18632/aging.205121.
[21] S. Shamas, R.R. Rahil, L. Kaushal, V.K. Sharma, N.A. Wani, S.H. Qureshi, S. F. Ahmad, S.M. Attia, M.A. Zargar, A. Hamid, O.M. Bhat, Pyroptosis in Endothelial Cells and Extracellular Vesicle Release in Atherosclerosis via NF-κB-Caspase-4/5-GSDM-D Pathway, Pharmaceuticals (Basel) 17 (12) (2024) 1568, https://doi.org/10.3390/ph17121568.
[22] J.H. Xing, R. Li, Y.Q. Gao, M.Y. Wang, Y.Z. Liu, J. Hong, J.Z. Dong, H.P. Gu, L. Li, NLRP3 inflammasome mediates palmitate-induced endothelial dysfunction, Life Sci. 239 (2019) 116882, https://doi.org/10.1016/j.lfs.2019.116882.
[23] Y. Zheng, L. Xu, N. Dong, F. Li, NLRP3 inflammasome: the rising star in cardiovascular diseases, Front. Cardiovasc. Med. 9 (2022) 927061, https://doi.org/10.3389/fcvm.2022.927061.
[24] S. Toldo, E. Mezzaroma, L.F. Buckley, N. Poter, M. Di Nisio, G. Biondi-Zoccai, B. W. Van Tassell, A. Abbate, Targeting the NLRP3 inflammasome in cardiovascular diseases, Pharmacol. Ther. 236 (2022) 108053, https://doi.org/10.1016/j.pharmthera.2021.108053.
[25] S. Gastaldi, C. Rocca, E. Gianquinto, M.C. Granieri, V. Boscaro, F. Blua, B. Rolando, E. Marini, M. Gallicchio, A. De Bartolo, N. Romeo, R. Mazza, F. Fedele, P. Pagliaro, C. Penna, F. Spyrakis, M. Bertinaria, T. Angelone, Discovery of a novel 1,3,4-

oxadiazol-2-one-based NLRP3 inhibitor as a pharmacological agent to mitigate cardiac and metabolic complications in an experimental model of diet-induced metaflammation, Eur. J. Med. Chem. 257 (202) (2023) 115542, https://doi.org/10.1016/j.ejmech.2023.115542.
[26] S. Gastaldi, M. Giordano, F. Blua, C. Rubeo, V. Boscaro, S. Femminò, S. Comità, E. Gianquinto, V. Landolfi, E. Marini, M. Gallicchio, F. Spyrakis, P. Pagliaro, M. Bertinaria, C. Penna, Novel NLRP3 inhibitor INF195: Low doses provide effective protection against myocardial ischemia/reperfusion injury, Vascul. Pharmacol. 156 (2024) 107397, https://doi.org/10.1016/j.vph.2024.107397.
[27] M. Giordano, S. Femminò, F. Blua, F. Boccato, C. Rubeo, B. Mantuano, F. Cioffi, S. Comità, A. Brovero, R. Ciullo, M. Bertinaria, C. Penna, P. Pagliaro, Macrophage and cardiomyocyte roles in cardioprotection: Exploiting the NLRP3 Inflammasome inhibitor INF150, Vascul. Pharmacol. 159 (2025) 107487, https://doi.org/10.1016/j.vph.2025.107487.
[28] Y. Shao, J. Saredy, W.Y. Yang, Y. Sun, Y. Lu, F. Saaoud, , C.4th Drummer, C. Johnson, K. Xu, X. Jiang, H. Wang, X. Yang, Vascular Endothelial Cells and Innate Immunity, Arterioscler. Thromb. Vasc. Biol. 40 (6) (2020) e138–e152, https://doi.org/10.1161/ATVBAHA.120.314330.
[29] L. Bellik, C. Musilli, M.C. Vinci, F. Ledda, A. Parenti, Human mature endothelial cells modulate peripheral blood mononuclear cell differentiation toward an endothelial phenotype, Exp. Cell Res. 314 (16) (2008) 2965–2974, https://doi.org/10.1016/j.yexcr.2008.07.016.
[30] P. Zhou, S. Lu, Y. Luo, S. Wang, K. Yang, Y. Zhai, G. Sun, X. Sun, Attenuation of TNF-α-Induced Inflammatory Injury in Endothelial Cells by Ginsenoside Rb1 via Inhibiting NF-κB, JNK and p38 Signaling Pathways, Front. Pharmacol. 8 (2017) 464, https://doi.org/10.3389/fphar.2017.00464.
[31] X. Deng, J. Zhang, Y. Liu, L. Chen, C. Yu, TNF-α regulates the proteolytic degradation of ST6Gal-1 and endothelial cell-cell junctions through upregulating expression of BACE1, Sci. Rep. 7 (2017) 40256, https://doi.org/10.1038/srep40256.
[32] C. Rocca, A. De Bartolo, R. Guzzi, M.C. Crocco, V. Rago, N. Romeo, I. Perrotta, E. M. De Francesco, M.G. Muoio, M.C. Granieri, T. Pasqua, R. Mazza, L. Boukhzar, B. Lefranc, J. Leprince, M.E. Gallo Cantafio, T. Soda, N. Amodio, Y. Anouar, T. Angelone, Palmitate-Induced Cardiac Lipotoxicity is Relieved by the Redox-active motif of SELENOT through improving Mitochondrial Function and Regulating Metabolic State, Cells 12 (7) (2023) 1042, https://doi.org/10.3390/cells12071042.
[33] M. Cecchi, C. Anceschi, A. Silvano, M.L. Coniglio, A. Chinnici, L. Magnelli, A. Lapucci, A. Laurenzana, A. Parenti, Unveiling the Role of Tryptophan 2,3-Dioxygenase in the Angiogenic Process, Pharmaceuticals (Basel) 17 (5) (2024) 558, https://doi.org/10.3390/ph17050558.
[34] D.A. Wink, K.M. Miranda, M.G. Espey, R.M. Pluta, S.J. Hewett, C. Colton, M. Vitek, M. Feelisch, M.B. Grisham, Mechanisms of the antioxidant effects of nitric oxide, Antioxid. Redox Signal. 3 (2) (2001) 203–213, https://doi.org/10.1089/152308601300185179.
[35] J.J. Liang, I.D.C. Fraser, C.E. Bryant, Lipid regulation of NLRP3 inflammasome activity through organelle stress, Trends Immunol. 42 (9) (2021) 807–823, https://doi.org/10.1016/j.it.2021.07.005.
[36] M. Rayamajhi, Y. Zhang, E.A. Miao, Detection of pyroptosis by measuring released lactate dehydrogenase activity, Methods Mol. Biol. 1040 (2013) 85–90, https://doi.org/10.1007/978-1-62703-523-1_7.
[37] S. Toldo, A. Abbate, The role of the NLRP3 inflammasome and pyroptosis in cardiovascular diseases, Nat. Rev. Cardiol. 21 (4) (2024) 219–237, https://doi.org/10.1038/s41569-023-00946-3.
[38] Z.H. Lv, T.A. Phuong, S.J. Jin, X.X. Li, M. Xu, Protection by simvastatin on hyperglycemia-induced endothelial dysfunction through inhibiting NLRP3 inflammasomes, Oncotarget 8 (53) (2017) 91291–91305, https://doi.org/10.18632/oncotarget.20443.
[39] T. Jiang, D. Jiang, L. Zhang, M. Ding, H. Zhou, Anagliptin ameliorates high glucose-induced endothelial dysfunction via suppression of NLRP3 inflammasome activation mediated by SIRT1, Mol. Immunol. 107 (2019) 54–60, https://doi.org/10.1016/j.molimm.2019.01.006.
[40] Y. Zhang, Y.T. Wang, S. Koka, Y. Zhang, T. Hussain, X. Li, Simvastatin improves lysosome function via enhancing lysosome biogenesis in endothelial cells, Front. Biosci. (landmark Ed) 25 (2) (2020) 283–298, https://doi.org/10.2741/4807.
[41] L. Shi, Y. Xu, C. Zhao, G. Qu, M. Hao, Liraglutide ameliorates high glucose-induced vascular endothelial injury through TRIB3/NF-κB signaling pathway, In Vitro Cell. Dev. Biol. Anim. 60 (9) (2024) 1046–1057, https://doi.org/10.1007/s11626-024-00947-7.
[42] L. Villacampa, I. Shamoon, C. Valencia, S. Morales, F. de la Figueiras, D. Cuesta, G. Sánchez-Niño, I. Díaz-Araya, Ó. Sánchez-Pérez, C.F. Lorenzo, C. Sánchez-Ferrer, Peiró, SARS-CoV-2 S Protein Reduces Cytoprotective Defenses and Promotes Human Endothelial Cell Senescence, Aging Dis. 16 (3) (2024) 1626–1638, https://doi.org/10.14336/AD.2024.0405.
[43] H. Zhang, H. Chen, X. Wu, T. Sun, M. Fan, H. Tong, Y. Zhu, Z. Yin, W. Sun, C. Zhang, X. Zheng, X. Chen, Tetramethylpyrazine alleviates diabetes-induced high platelet response and endothelial adhesion via inhibiting NLRP3 inflammasome activation, Phytomedicine 96 (2022) 153860, https://doi.org/10.1016/j.phymed.2021.153860.
[44] H. Yang, L. Xiao, Y. Yuan, X. Luo, M. Jiang, J. Ni, N. Wang, Procyanidin B2 inhibits NLRP3 inflammasome activation in human vascular endothelial cells, Biochem. Pharmacol. 92 (4) (2014) 599–606, https://doi.org/10.1016/j.bcp.2014.10.001.
[45] J. Lv, S. Shi, B. Zhang, X. Xu, H. Zheng, Y. Li, X. Cui, H. Wu, Q. Song, Role of puerarin in pathological cardiac remodeling: a review, Pharmacol. Res. 178 (2022) 106152, https://doi.org/10.1016/j.phrs.2022.106152.
[46] H. Wei, M. Sun, R. Wang, H. Zeng, B. Zhao, S. Jin, Puerarin mitigated LPS-ATP or HG-primed endothelial cells damage and diabetes-associated cardiovascular disease via ROS-NLRP3 signalling, J. Cell Mol. Med. 28 (10) (2024) e18239, https://doi.org/10.1111/jcmm.18239.